

Technologies and Materials for Renewable Energy, Environment & Sustainability

Electrospun Polycaprolactone/Polyethylene Oxide Blends with Optimal Conditions for Scaffold Application

AIPCP25-CF-TMREES2025-00057 | Article

PDF auto-generated using **ReView**



Electrospun Polycaprolactone/ Polyethylene Oxide Blends With Optimal Conditions for Scaffold Application

Ali Hameed ^{1, a}, Manar Najim ^{1, b}, Akram Jabur ^{1, c}

¹ College of Materials Engineering, University of Technology- Iraq.

^{a)} Corresponding author: 130216@uotechnology.edu.iq

^{b)} manar.a.najim@uotechnology.edu.iq

^{c)} akram.r.jabur@uotechnology.edu.iq

Abstract. This study investigates the fabrication and characterization of electrospun scaffolds made from varying proportions of polycaprolactone (PCL) and polyethylene oxide (PEO). The study explains how electrospinning parameters (polymer concentration and voltage) affect the chemical and physical features of PCL/PEO blends. The optimum conditions and concentrations for these blends are found to be suitable for medical applications as scaffolds or drug delivery systems. The mixture of PCL and PEO was dissolved in chloroform to create homogeneous solutions. The electrospinning technique was used to fabricate fibrous mats, which were analyzed for their physical and chemical characteristics. The wettability of the fibrous mat surfaces was assessed using the contact angle. The study found that increasing PEO concentration to 3% in the blend specimen electrospun at 25 KV voltage enhanced membrane wettability and produced more homogeneous fibrous structures, facilitating the creation of biocompatible materials for soft tissue regeneration. The Fourier Transform Infrared Spectroscopy (FTIR) results showed that the strength of the PCL characteristic peaks got weaker as the PEO concentrations increased.

Keywords: Polyethylene Oxide, Polycaprolactone, Electrospinning, Nanofibers, Scaffold.

INTRODUCTION

Electrospinning is a popular method for producing nanofibers, particularly for biomedical applications. It involves injecting a polymeric solution into a syringe, which is then pumped with high voltage. This electric force exceeds the solution's viscoelastic force, resulting in the ejection of a solution jet. This technology forms thin fibrous structures, making it adaptable and effective in various applications [1]. Polycaprolactone (PCL) is a biodegradable, blend-compatible, thermoplastic, semi-crystalline, and nonimmunogenic polymer used in biomedical applications due to its unique properties. Its solubility in various solvents makes it a viable substitute for conventional plastics [2]. Polyethylene oxide (PEO), a soft semi-crystalline thermoplastic material, is used in controlled-release tablet systems for prolonged drug release, enhancing therapeutic effects and patient adherence [3]. Combining PCL with PEO enhances its properties, broadens its applicability in tissue engineering, and exhibits biodegradability and mechanical properties. The combination of PCL and PEO polymers improves mechanical strength, flexibility, surface characteristics, and biocompatibility attributed to the inclusion of PEO [4]. To create electrospun PCL/PEO membranes, Yan-Fang Li et al explored the use of binary polymer blends, specifically PCL and PEO, to create unique fibers with distinctive properties [5]. Melda Eskitoros-Togay et al synthesized electrospun membranes for drug delivery applications by blending PCL and PEO with doxycycline, using dichloromethane and N, N-dimethylformamide solvents [6]. Zeynab Mirzaei et al blended PCL and PEO with chloroform solvent to create electrospun fibers for potential cartilage regeneration applications [7]. Maurice Dalton et al developed PCL/PEO blends for soft tissue engineering, adjusting degradation kinetics by altering PEO molecular weights with improved hydrophilicity and reduced melt viscosity, making them suitable for soft tissue applications [8]. This study aims to evaluate the effect of changing applied voltage and PEO concentration in improving the [PCL: PEO] electrospun blend scaffold structure and wettability to reach optimized properties for tissue applications.

EXPERIMENTAL SECTION

Materials

Polycaprolactone (PCL), exhibiting an average molecular weight (Mw) of 80,000 Da, was purchased from Sigma-Aldrich, United Kingdom, under product no. 440744. Polyethylene oxide (PEO) with an average molecular weight (Mw) of 600,000 Da was purchased from Thermo Scientific Fisher in Japan, under product no. A0449511. In addition, chloroform with Hi-AR (>99.0%) was obtained from HIMEDIA, India.

METHODS

Preparation of Fibers

A PCL solution was prepared by dissolving it in chloroform at a 15% w/v concentration, while three different concentrations of PEO were prepared from 1% to 3%. To evaluate the effect of increasing PEO concentrations on blend scaffold structure and wettability, three solutions of [50:50] [PCL: PEO] were prepared. The blend solutions were stirred on a magnetic stirrer for 2 hours, and ultrasonication was applied for 3 minutes to achieve homogeneous blends. Electrospinning was applied according to the specified parameters outlined in Table 1, utilizing a stainless-steel flat plate collector and a needle orifice size of 22G (0.7 mm). The distance between capillary and collector was 20 cm, and the flow rate was 1 mL/hr for all specimens. The electrospinning process was conducted at room temperature.

Table 1. Specimens Nomenclature with their electrospinning parameters.

Membrane	Specimen	Voltage (KV)
M1	Pure PCL 15%	15
M2	Pure PCL 15%	25
M3	Pure PEO 1%	15
M4	Pure PEO 1%	25
M5	Pure PEO 2%	15
M6	Pure PEO 2%	25
M7	Pure PEO 3%	15
M8	Pure PEO 3%	25
M9	[50:50] PCL 15%, PEO 1%	15
M10	[50:50] PCL 15%, PEO 1%	25
M11	[50:50] PCL 15%, PEO 2%	15
M12	[50:50] PCL 15%, PEO 2%	25
M13	[50:50] PCL 15%, PEO 3%	15
M14	[50:50] PCL 15%, PEO 3%	25

Scanning Electron Microscope (SEM) Characterization

Characterization of surface morphology for the fabricated specimens (M1-M14) was conducted using scanning electron microscopy (SEM; FEI Company, Inspect™ F50, USA) at an accelerated voltage of 30 kV and a working distance of 10 mm. prior to the observation, the specimens underwent sputter-coating with gold in a vacuum environment to prevent charges from accumulating [9].

Statistical Analysis

The analysis of SEM images was conducted using Image J software 1.54g version analysis (Maryland, USA), focusing on the measurement of 50 distinct fibers from each SEM image of the fabricated membranes. Subsequently, we determined the average fiber diameter and its standard deviation utilizing Microsoft Excel [10].

Contact Angle Measurements

The contact angle of fibrous mat specimens was measured using ASTM standard D 5946-04. The specimens were placed on a testing plate and 0.03 mL of distilled water was applied to the surface. Three measurements were documented, with results presented as average \pm SD. The results were presented as average \pm SD immediately following the droplet's release

Fourier Transform Infra- Red Spectroscopy FTIR Characterization

Fourier transform infrared (FTIR) spectroscopy (Type of spectrometer, Tensor 27, Germany- Bruker Optik system) was applied to examine fabricated membranes in the wave number range of $4000\text{--}400\text{ cm}^{-1}$ and a KBr beam splitter in transmission mode. The obtained spectra were analyzed to identify functional groups and chemical bonds present in pure and blend membranes, providing insights into their molecular structure and composition.

RESULTS AND DISCUSSION

SEM and Statistical Analysis Measurements

To study the structure of electrospun SEM imaging was used to examine the structure of electrospun pure and blended specimens. The specimens (M1 and M2) were processed at 15 kV and 25 kV, revealing a smooth surface without bead formation. M1 had a range of fiber diameters, with an average diameter of $2204.24 \pm 1321.91\text{ nm}$ and a high standard deviation. M2 had a lower average diameter and standard deviation, indicating a more uniform fiber distribution, as shown in Figure 1. The reduction in average diameter after increasing voltage was attributed to increased conductivity, leading to more fiber elongation and reduced diameter. This finding was also confirmed by Najim et al [11]. Pure PEO solutions of different concentrations were electrospun at two voltages (15 and 25 KV). At 15 KV, increasing the concentration of PEO led to an increased average fiber diameter with non-uniform structures, as shown in Figure 2. In the M3 specimen the average fiber diameter was $1107.37 \pm 671.57\text{ nm}$, which increased to $2691.05 \pm 814.48\text{ nm}$ and $7466.38 \pm 1373.27\text{ nm}$ in the M5 and M7 specimens, respectively, and the last two specimens also showed non-uniform fibrous structures. In electrospinning, higher concentration or molecular weight leads to the production of thicker fibers, as reported by Manar et al [12].

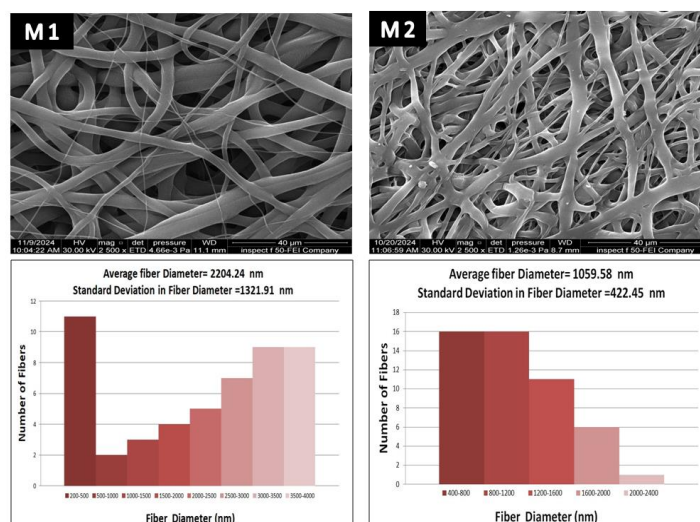


Figure 1. SEM images of M1 and M2 specimens.

Pure PEO samples had a smaller average fiber diameter when a voltage of 25 KV was used, just like pure PCL, as shown in Figure 3. M4 and M6 specimens had tangled fiber structures that were not uniform, with average diameters

of 1103.66 ± 669.61 nm and 1994.25 ± 334.74 nm, respectively. The applied voltage can impact fiber beading and entanglement due to jet instabilities at high voltages [13]. However, the M8 specimen with 3% w/v PEO had a consistent fiber structure with an average diameter of 2057.87 ± 300.65 nm, unlike the M7 specimen made at a lower voltage (15 KV). This variation is due to the stability in the Taylor cone and spinning jet columbic repulsive forces, extending the high-concentration viscoelastic solution. However, increasing the applied voltage should not exceed the critical limit for drops from the needle tip and bead formation, as proven by Akram and Ali [14]. Mixing PCL with PEO in a [50:50] [PCL: PEO] ratio using 1% to 3% w/v PEO concentrations created more even and consistent fibrous structures compared to pure PEO samples. Figure 4 showed SEM images of the blended specimen's electrospun at 15 KV. These specimens had larger average fiber diameters of 6316.67 ± 624.127 nm, 5523.51 ± 1308.22 nm, and 2489.4 ± 871.241 nm for M9, M11, and M13, respectively. However, increasing the applied voltage to 25 KV during the electrospinning of M10, M12, and M14 specimens revealed a decrease in fiber diameter and uniformity in fibrous structures, as depicted in Figure 5. The smallest average fiber diameter with the most uniformity in the blended specimens was recorded in M14 specimen 1465.96 ± 569.78 nm. The findings from the blended specimens indicated that increasing PEO concentrations resulted in a reduction in average fiber diameter, whereas in pure PEO the addition of voltage led to an increase in fiber diameter. This observation aligns with the work of Ribeiro et al, who noted that as the concentration of PEO increases, there are corresponding changes in the viscosity and conductivity of the polymer solution, which may initially produce larger fiber diameters. However, when PEO is mixed with other polymers, the way they interact can greatly change these properties and lead to a smaller fiber diameter.

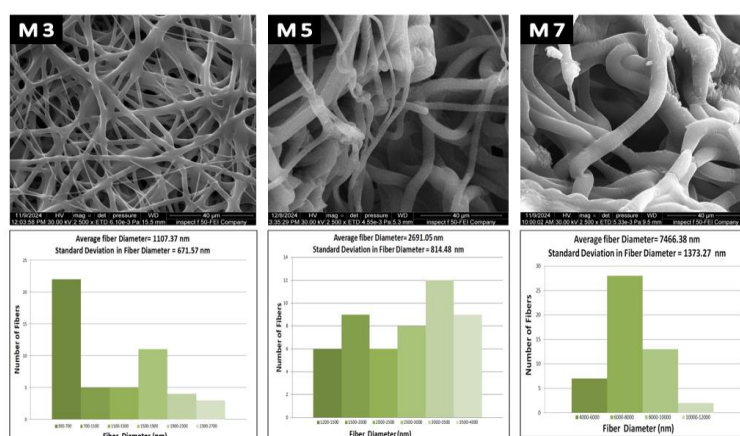


Figure 2. SEM images of M3, M5 and M7 specimens.

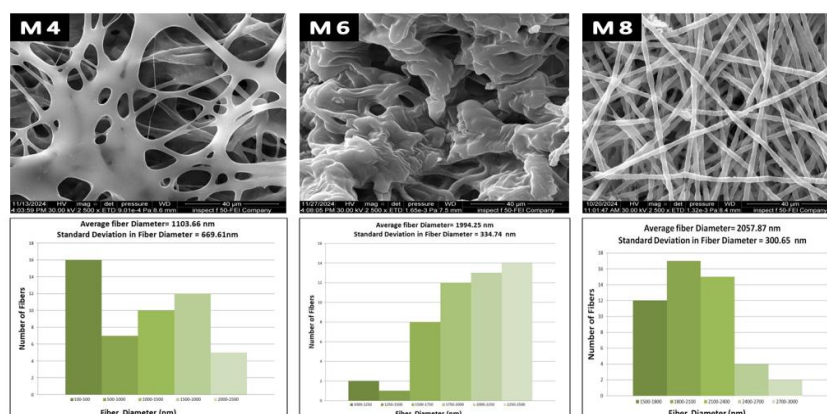


Figure 3. SEM images of M4, M6 and M8 specimens.

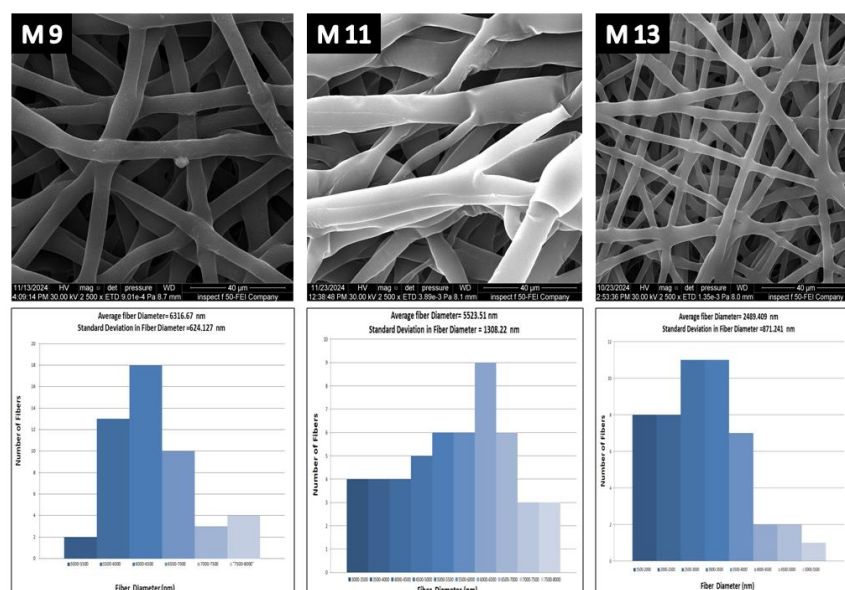


Figure 4. SEM images of M9, M11 and M13 specimens.

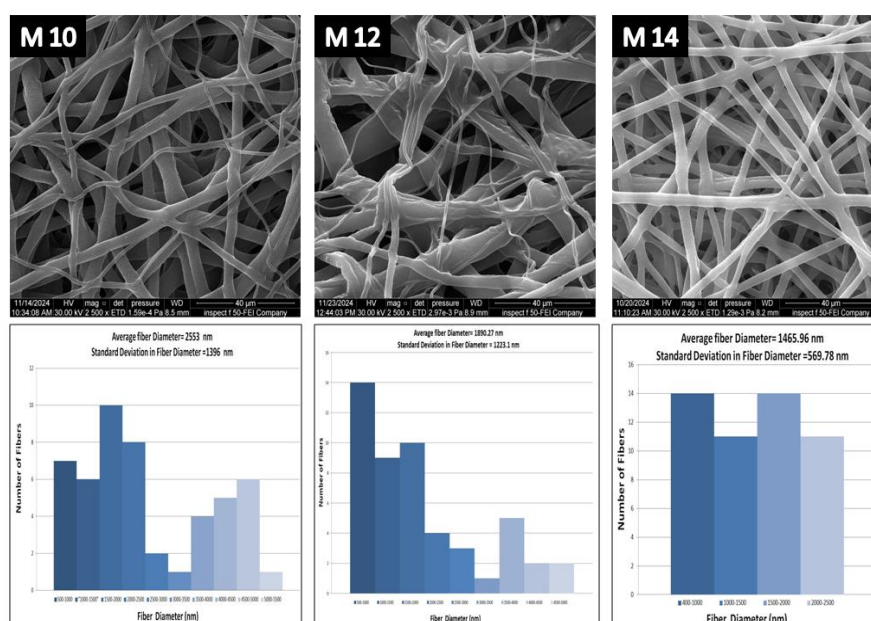


Figure 5. SEM images of M10, M12 and M14 specimens.

Contact Angle Measurements

The wettability of fibrous mats significantly influences their interaction with liquids, particularly in tissue engineering applications. PCL is a hydrophobic polymer [7], while PEO is hydrophilic due to hydrophilic functional groups in its structure [7]. Images of water contact angles are shown in Figures 6 and 7. As expected, increasing PEO concentration in the blend altered the membrane's characteristics from hydrophobic to hydrophilic.

Consequently, M1, M2, and M9 specimens exhibited poor wettability attributed to the pure PCL or a lower percentage of PEO, whereas M3 to M8 demonstrated a hydrophilic nature because of pure PEO content. Between the blend specimens, M13 and M14 exhibited remarkable hydrophilicity, attributed to the higher concentration of PEO with polar hydroxyl groups. The investigation conducted by Li et al regarding PCL and PEO electrospun membranes revealed that incorporating PEO resulted in a decreased water contact angle value [16].

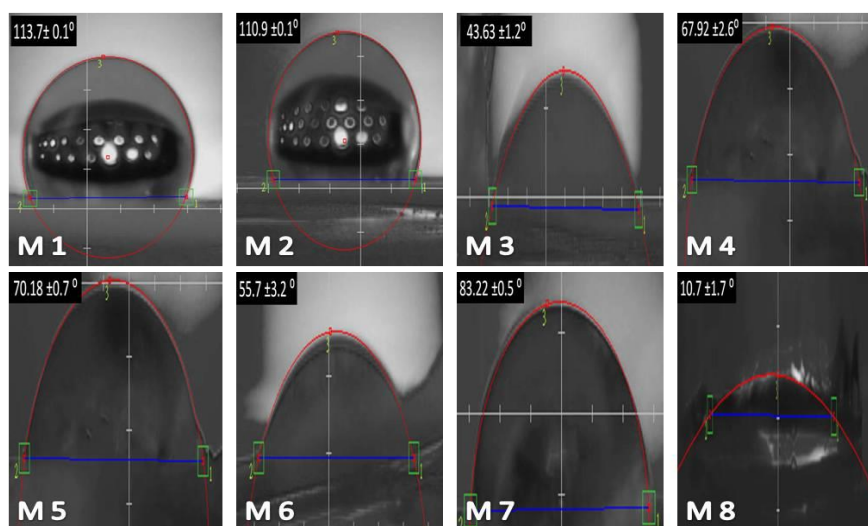


Figure 6. Water contact angles of M1-M8 specimens.

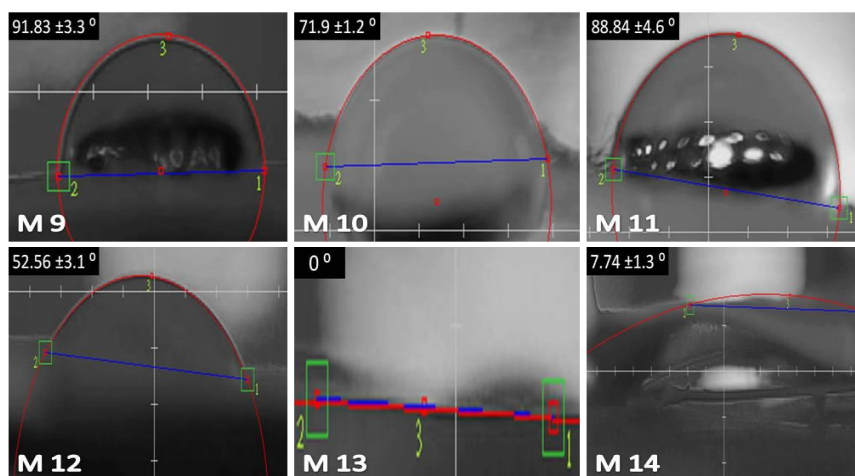
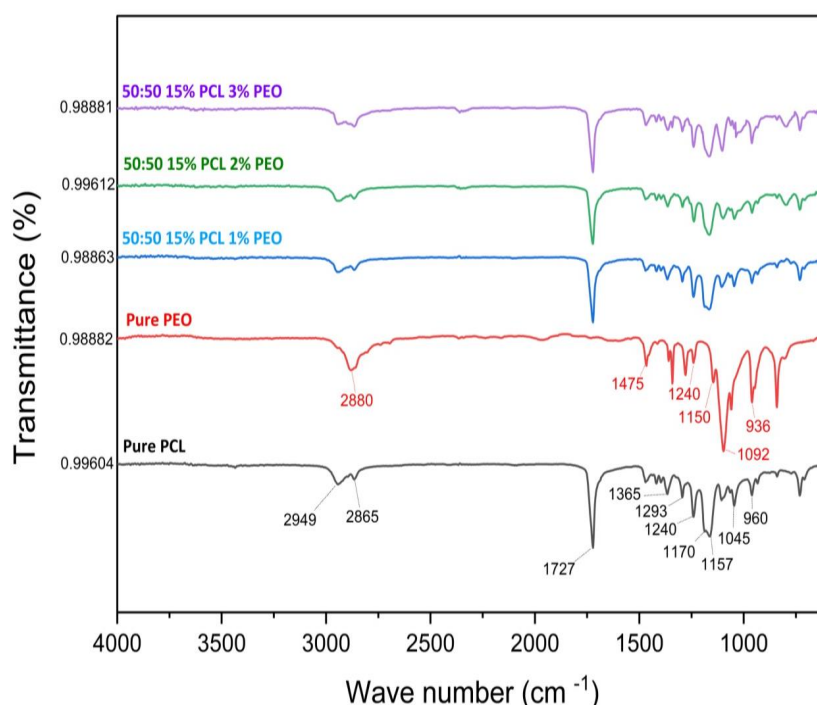


Figure 7. Water contact angles of M9-M14 specimens.

FTIR Measurements

FTIR spectroscopy is used to identify all significant peaks in the FTIR spectra of pure PCL and PEO across different blend concentrations. The characteristic peaks of PCL included bending vibrations of certain bonds, such as C-H bending at 960 cm^{-1} , C-O stretching and vibrations at 1045 cm^{-1} , C-O at 1157 cm^{-1} , symmetric COC stretching at 1170 cm^{-1} , C-O stretching vibrations that related to the ester groups in the polymer at 1240 cm^{-1} , and C-C stretching at 1293 cm^{-1} . The presence of a peak at 1365 cm^{-1} could indicate various functional groups such as C-H bending vibrations. A strong peak around 1727 cm^{-1} corresponds to the carbonyl C=O stretching vibration,

which is the characteristic peak of PCL. Peaks near 2865 cm^{-1} are attributed to the stretching vibrations of C-H bonds from the methylene ($-\text{CH}_2$) groups present in PCL, and asymmetric CH_2 at 2949 cm^{-1} [17]. The FTIR spectra of pure PEO revealed peaks at 963 cm^{-1} , 1092 cm^{-1} , 1150 cm^{-1} , 1240 cm^{-1} , 1475 cm^{-1} , and 2880 cm^{-1} , which correspond to the characteristic vibrations of CH_2 groups, as well as the symmetric and asymmetric stretching vibrations of C-O-C, which is the characteristic peak of PEO, C-O stretching, bending vibrations of CH_2 groups, and C-H stretching, respectively [18]. The relative intensity of the characteristic peaks of PEO increased with a higher ratio of PEO to PCL. Additionally, the peak at 1727 cm^{-1} , which is a key feature of PCL, showed a weaker intensity as more PEO was added to the mixture, as noted by Mirzaei. The intensity of the C-H peaks at 2880 cm^{-1} increased in blends of different concentrations compared to pure PCL, as PEO also features a C-H bond at this wavelength. Nevertheless, the intensity was elevated in all blend specimens. The decrease in the intensity of PCL's characteristic peaks, along with the increase in the intensity of PEO's characteristic peaks as PEO concentrations rose, indicates that a successful blending process occurred between these two polymers, particularly since no new peaks appeared. This was consistent with Mirzaei et al who also did not recognize the new peak appearance and concluded successful compounding between PCL and PEO [11].



Figures 8. FTIR for pure polymers and their blends

CONCLUSIONS

This work studied the improvement of the [PCL: PEO] blend to adjust their wettability and structure to be used in medical applications, like scaffolds and drug delivery systems. Increasing the amount of PEO to 3% w/v in the blend samples made them wetter and created a smooth, fibrous structure, especially when the voltage was raised to 25 KV in the M14 sample. The high voltage used made the blend solutions with 3% w/v PEO stretch more, which made the fibers thinner and prevented beads from forming. Also, using ultrasonication during solution preparation resulted in advanced homogeneity in blend solutions. When the amount of PEO is increased, the strength of its unique signals goes up while the strength of the unique signals from PCL goes down, confirming that PCL and PEO are blending well together.

REFERENCES

1. Subbiah, T., Bhat, G. S., Tock, R. W., Parameswaran, S., & Ramkumar, S. S, *Journal of Applied Polymer Science*, **96**(2), 557–569 (2005).
2. Correa, A. C., Carmona, V. B., Simão, J. A., Mattoso, L. H. C., & Marconcini, J. M, *Carbohydrate Polymers*, **167**, 177–184 (2017).
3. M.A. Najim, R.R. Ayoob, and A.A. Hameed, *Heliyon* **10**(15), e35640 (2024).
4. Kennedy, S. W., Choudhury, N. R., & Parthasarathy, R, *Bioprinting*, **30**, e00259 (2023).
5. Li, Y., Rubert, M., Aslan, H., Yu, Y., Howard, K. A., Dong, M., Chen, M, *Nanoscale*, **6**(6), 3392, (2014).
6. Eskitoros-Togay, Ş. M., Bulbul, Y. E., Tort, S., Korkmaz, F. D., Acartürk, F., & Dilsiz, N, *International Journal of Pharmaceutics*, **565**, 83–94, (2019).
7. Mirzaei, Z., Kordestani, S. S., Kuth, S., Schubert, D. W., Detsch, R., Roether, J. A., Boccaccini, A. R, *Advanced Engineering Materials*, **22**(9), (2020).
8. Dalton, M., Ebrahimi, F., Xu, H., Gong, K., Fehrenbach, G., Fuenmayor, E., Major, I, *Macromol—A Journal of Macromolecular Research*, **3**(3), 431–450, (2023).
9. Chayad, F. A., Jabur, A. R., & Jalal, N. M, *Engineering and Technology Journal*, **34**(7), 1265–1274, (2016).
10. Khalil, S., Ibrahim, S., Al-Juboori, R., Lau, W., Low, S., Jawad, Z., Alsahy, Q, *Engineering and Technology Journal*, **0**(0), (2025).
11. M.A. Najim, B.I. Khalil, and A.A. Hameed, *Heliyon* **8**(11), e11423, (2022).
12. M.A. Najim, A.R. Jabur, and A.A. Hameed, *Materials Science Forum*, **1002**, 84–94, (2020).
13. A. Jabur, *Engineering and Technology Journal*, **38**(3A), 431–439, (2020).
14. A.R. Jabur, and A.A. Hameed, *12th International Conference on Developments in eSystems Engineering (DeSE)* **34**, 750–754, (2019).
15. C. Ribeiro, V. Sencadas, C. Caparros, J.L.G. Ribelles, and S. Lanceros-Méndez, *Journal of Nanoscience and Nanotechnology*, **12**(8), 6746–6753, (2012).
16. C. Li, Z.-H. Wang, and D.-G. Yu, *Colloids and Surfaces B Biointerfaces*, **114**, 404–409, (2013).
17. S.B. Qasim, S. Najeeb, R.M. Delaine-Smith, A. Rawlinson, and I.U. Rehman, *Dental Materials* **33**(1), 71–83, (2016).